A R C H I V E S O F M E T A L L U R G Y A N D M A T E R I A L S
Volume 51 2006 Issue 3

D.V. HERNANDEZ* , A.F. VALDES*

A KINETIC STUDY ON THE MAGNESIUM REMOVAL FROM MOLTEN ALUMINUM USING Ar-SF6-O2 GASEOUS MIXTURES

BADANIA KINETYKI USUWANIA MAGNEZU Z ALUMINIUM PRZY UŻYCIU GAZOWYCH MIESZANIN Ar-SF6-O2

In this paper it is shown that pneumatically injected gaseous mixtures containing $SF_6(g)$ are useful to oxidize the magnesium dissolved in molten aluminum alloys. Although the oxidation of magnesium with $SF_6(g)$ is thermodynamically favorable, the addition of $O_2(g)$ causes that ΔG is additionally reduced by −249.16 KJ/mol Mg. After chemical analysis of the final contents of magnesium in the treated alloys, the identification of compounds in the slag by x-ray diffraction, and chemical analysis of gaseous emissions produced, a scheme of reaction is proposed. A kinetic model describing the magnesium removal rate is presented, taking into account that kinetics of the process is controlled by chemical reaction.

W artykule przedstawiono wyniki badań nad wykorzystaniem gazowych mieszanin zawierających SF_6 do utleniania magnezu rozpuszczonego w stopach aluminium. Chociaż utlenianie magnezu przez czysty SF_6 charakteryzuje ujemna wartość ΔG, dodatek O_2 w mieszaninie gazowej powoduje dodatkową redukcję ΔG o wartość −249.16 kJ/mol Mg. Próbki stopów aluminium oczyszczanych z magnezu przy użyciu mieszanin Ar-SF_6-O2 były poddawane analizie chemicznej (atomowy spektrometr emisyjny) na zawartość magnezu, a następnie po zakończeniu procesu analizowane pod kątem identyfikacji związków chemicznych metodą rentgenowskiej analizy dyfrakcyjnej. Skład gazów emitowanych podczas prób laboratoryjnych był także badany. Na podstawie wyników badań zaproponowano schemat reakcji utleniania magnezu oraz model kinetyczny przebiegu procesu usuwania magnezu ze stopów aluminiowych przy założeniu, że szybkość procesu jest kontrolowana szybkością procesów chemicznych.

1. Introduction

Gas injection from porous diffusers has been widely used in molten metal refining. The pneumatic injection of binary gaseous mixtures composed of Cl_2/Ar or Cl_2/N_2 allows not only enhancing mixing conditions but also the oxidation and removal of alkali and alkaline-earth metals from molten aluminum. Moreover, the elimination of hydrogen implicitly occurs [1]. However, due to the highly corrosive effects of chlorine bubbling, the use of argon based gaseous mixtures containing low amounts of $O_2(g)$ and $SF_6(g)$ are suitable. Recently, the reactivity of $SF_6(g)$ has been studied in removing arsenic, antimony and bismuth from molten copper alloys [2]. Other investigations demonstrate that gaseous mixtures composed of SF_6, O_2, and Ar, are useful to reduce the magnesium content from molten aluminum alloys [3]. Table 1 contains the set of chemical reactions that are believed to take place when using these gaseous mixtures for molten aluminum refining. The theoretical thermodynamic results were calculated using the software from Outokumpu, HSC Chemistry for Windows. This software allows the obtention of the values of the Gibbs free energy for all reactions proposed as well as the values of the equilibrium constants [4].

A result that justifies the use of SF_6-O_2 gaseous mixtures for refinement of aluminum scrap is obtained analyzing the values of equilibrium constants and Gibbs free energies of the reactions R4 and R6 from Table 1 at 1000 K, taking the activity coefficient of magnesium equal to 1. From the values reported, it could be stated that reaction R6 is favored with respect to reaction R4 due to a difference in the Gibbs free energy equal to −249.16 KJ per mole of Mg. Therefore, the oxidation of pure magnesium would be high when the composition of the gaseous mixture reaches a molar ratio 1:1 for $O_2(g)$ and $SF_6(g)$.

On the other hand, the dispersion of a gaseous phase inside a liquid one has been extensively studied for Air-H_2O physical models [5]. The experimental results have shown that the size of gas bubbles depends on the

* CINVESTAV-IPN UNIDAD SALTILLO, SALTILLO-MONTERREY HIGHWAY KM. 13.5, 25900, RAMOS ARIZPE, COAHUILA, MÉXICO

area of the diffuser, average pore diameter and gas flow rate. The mixing power input per kilogram of molten metal is also a useful parameter to determine the fluidynamic conditions to refine a mass of metal on a given scale. Therefore, for scaling up purposes it is important to characterize the conditions imposed during pneumatic injection of gaseous mixtures.

In this sense, the objective of this paper is to present the results of a kinetic study performed to refine magnesium from a molten aluminum alloy processed from scrap, using Ar/SF_6-O_2 gaseous mixtures. Characteristic values of molten metal stirring conditions achieved by pneumatic injection through a porous plug are also provided.

2. Experimental procedure

Figure 1 show the experimental equipment used in this work. It is composed of an electrical resistances furnace holding a SiC crucible 40 kg molten metal capacity. For refining experiments an Al-7Si-2Cu alloy containing around 1.0 wt. % Mg (±0.18 wt. %) was melted at 1023 K, before pneumatic injection of Ar-SF_6-O_2 gaseous mixtures initiated. The average amount of molten alloy in most experiments was of 21 kilograms (±1.0 Kg). The gaseous mixtures were delivered from cylindrical steel reservoirs provided by PRAXAIR México. The capacity of these cylinders was 0.049 m^3. The chemical composition, in mole fraction of each compound in the mixtures, is shown in Table 2. This Table includes some values of interest related to the fluid and mass flow conditions used during injection. Also, it gives the values of some of the thermophysical properties of the gaseous mixtures that were used to determine some values characterizing the mixing conditions imposed during pneumatic injection experiments. The injection pressure and gas flow rate were adjusted properly to ensure a treatment time delivering the specific molar amounts of $O_2(g)$ and $SF_6(g)$ according to the stoichiometry of the corresponding reactions proposed in Table 1. As it can be seen from Table 2, injection time varied depending on the chemical composition of the gaseous mixtures.

Pneumatic injection of the gaseous mixtures was done through lance 1 that consisted of a cladding made of pure alumina over a steel tube 0.635 mm in diameter. The end of this lance consisted of a diffuser made of high purity alumina with a density near to 96% of the theoretical density [6].

The basic dimensions of this lance were a height of 0.96 m and a total area of diffuser of 0.03 m^2. Lance 2 was used in some experiments to deliver an argon flow over the surface of the molten metal to prevent excessive oxidation by the surrounding atmosphere.

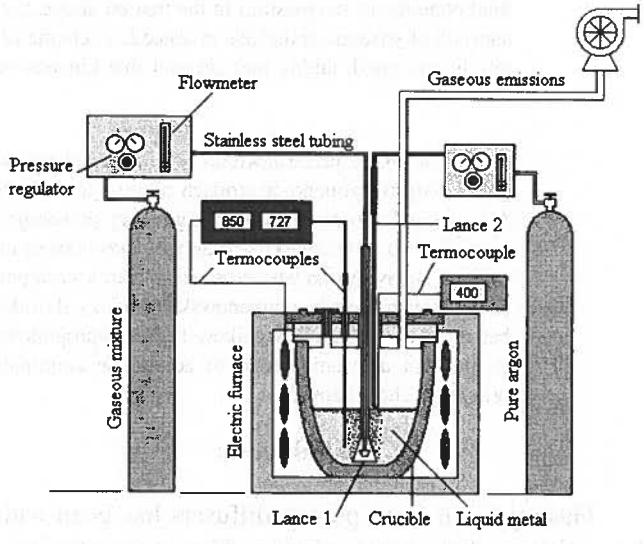

Fig. 1. Scheme of the experimental set-up used in this work

TABLE 1

Reactions suggested, the values of Gibbs free energy and of the equilibrium constants calculated with HSC, corresponding to the oxidation of pure Al(l) and Mg(l) at 1000 K by Ar/SF_6-O_2 gaseous mixtures

Reaction	Metal oxidation reactions	ΔG_{1000K} (KJ/mole)	K_{Eq}
R1	$4/3\ Al(l) + O_2(g) \rightarrow 2/3\ Al_2O_3$	−906.91	2.37×10^{47}
R2	$O_2(g) + 2\ Mg(l) \rightarrow 2\ MgO$	−985.63	3.07×10^{51}
R3	$SF_6(g) + 4/3\ Al(l) \rightarrow 4/3\ AlF_3 + 1/3\ SF_4(g) + 1/3\ SSF_2(g)$	−1144.98	6.49×10^{59}
R4	$SF_6(g) + 2\ Mg(l) \rightarrow 2\ MgF_2 + 1/3\ SF_4(g) + 1/3\ SSF_2(g)$	−1378.88	1.07×10^{72}
R5	$SF_6(g) + O_2(g) + 4/3\ Al(l) \rightarrow SO_2F_2(g) + 4/3\ AlF_3$	−1394.14	6.73×10^{72}
R6	$SF_6(g) + O_2(g) + 2\ Mg(l) \rightarrow SO_2F_2(g) + 2\ MgF_2$	−1628.04	1.11×10^{85}
R7	$MgO + Al_2O_3 \rightarrow MgAl_2O_4$	−13.55	5.23
R8	$SF_6(g) + Al(l) + Mg(l) \rightarrow 1\ SSF_2(g) + MgF_2 + AlF_3$	−1540.67	3.04×10^{80}

TABLE 2
Chemical composition, the values of some parameters defining fluid and mass flow conditions, and the values of some thermo-physical properties of the gaseous mixtures

Gaseous mixture number	**03**	**06**	**13**	**14**
Molecular weight [g/mole]	31.17	37.68	18.21	42.07
Injection pressure [KPa]	121.30	500	500	500
Gaseous mixture density [Kg m^{-3}]	1.516	7.55	3.65	8.43
Gas flow rate[L/min]	1.50	20.00	20.00	20.00
Specific input power density [W/Kg]	0.025	1.38	1.38	1.38
Molar flow rate of gas [mole/s]	1.2E-03	0.067	0.067	0.067
Mole fraction of Ar [g]	0.80	0.88	0.90	0.98
Mole fraction of O2 [g]	0.20	0.10	0.0	0.00
Mole fraction of SF_6 [g]	0.00	0.02	0.10	0.02
Molar flow rate of Ar [mole/s]	7.3E-04	0.052	0.055	0.066
Molar flow rate of O_2 [mole/s]	2.4E-04	0.0067	0.00	0.00
Molar flow rate of SF_6 [mole/s]	0.00	0.0013	0.0067	0.0016
Injection time [s]	3583	3608	3642	4800
Mass injected of Ar [mole]	2.62	187.62	200.31	316.80
Mass injected of O_2 [mole]	0.86	24.17	0.00	0.00
Mass injected of SF_6 [mole]	0.000	4.69	24.40	6.24
Thermo-physical properties at 600K				
Kinematic viscosity at 500KPa [m^2 s^{-1}]	–	1.01E-05	1.90E-05	9.18E-06
Thermal conductivity at 500KPa [J $m^{-1}K^{-1}s^{-1}$]	–	0.041	0.174	0.031
Heat capacity at 500KPa [J $Kg^{-1}K^{-1}$]	–	644.03	1788.80	550.10
Dynamic viscosity at 500KPa [N s m^{-2}]	–	3.85E-05	3.46E-05	3.87E-05

Once the pneumatic injection initiated, samples from the melt were taken every 5 minutes up to achieve the treatment time for a specific gaseous mixture. The samples obtained were used to perform chemical analysis determining the actual concentration of magnesium. This was done by atomic emission spectrometry, following the standard procedure ASTM-E1251-94 [7]. Samples of slag were also taken at the end of each experiment, being prepared for examination by ray-X diffraction. The equipment utilized was a Philips Difractometer model PW 3040, with λ = 1.54056 Å. The scan velocity was 0.001 °/2θ.

Finally, Figure 1 also shows tubing line connected to a gas extraction system aimed to capture gaseous emissions released during experiments. A hole located just after the extractor served to introduce a quartz probe taking the amount of gas required for chemical analysis. Quantitative analysis of gaseous emissions, i.e. H_2S(g), HF(g) and SO_2(g), was made with a Bacharach Inc.® Model PCA55 gas analyzer equipment.

3. Results and Discussion

3.1. Analysis of stirring of the molten metal and estimation of bubbles size leaving from the diffuser

In order to have a consistent measure of the effects of the fluidynamic conditions on reaction rate for purposes of scaling up the refining process, it was necessary to calculate the values of some parameters characterizing gas dispersion and bubbles size in the system studied. However, owing to difficulties in examining the dispersion of gas bubbles in molten aluminum, some expressions were taken from studies related to the Air-H_2O system [5, 8–9]. According to the geometry of the accessories for pneumatic injection used in this work, the values of the parameters characterizing argon dispersion inside molten aluminum were calculated and are given in Table 3.

TABLE 3
The values of some parameters related to the dispersion of argon bubbles in molten aluminum corresponding to this work

Bubble size (average) d_B [m]	0.015
Ascending velocity of bubble [m/s]	0.5 ± 0.1
Superficial velocity of gas u_g [m/s]	0.051
Diffuser porosity ε [without dimensions]	0.34
Pore diameter d_{pm} (average) [μm]	69.3
Argon density (600K, 100Kpa) [Kg/m^3]	0.80058
Molten metal density ρ_L (aluminum) [Kg/m^3]	2354.0
Molten metal surface tension σ_L [N/m]	0.8 ± 0.1
Injection pressure P [KPa]	500.0
Atmospheric pressure P_a [Kpa]	101.325
Metalostatic pressure P_m [Kpa]	105.597
Molten metal depth H_L (average) [m]	0.185
Molten metal mass (average) m_L [Kg$_m$]	21.0 ± 1
Gas temperature at the inlet T_g [K]	600
Mixing power input [W/Kg$_m$]	1.38

From a comparison of dynamical analysis results about gas dispersion and stirring conditions in the systems Ar-Al and Air-H_2O, it is possible to define the fluid flow conditions imposed during injection in this work, using equations (1) through (6) given below. Since the values of Fr/We$^{0.5}$ in both systems must be the same, the numerical values of the expressions (4) and (5) are based on actual injection conditions and melt physical properties. Using an analytical procedure reported elsewhere [10], it was possible to develop a final expression for the size of bubbles in molten aluminum as represented by Eq. (6).

$$Q_g = (P_a/P_m) \cdot Q_{gN} \tag{1}$$

$$P_m = P_a + \rho_L g H_L \tag{2}$$

$$u_g = Q_g/A_n \tag{3}$$

$$\mathrm{Fr} = u_g^2/(\varepsilon^2 g d_{pm}) \tag{4}$$

$$\mathrm{We} = u_g^2 d_{pm}\rho_L/(\varepsilon^2 \sigma_L) \tag{5}$$

$$d_B = 0.0209\left(d_{pm}\sigma_L/g\rho_L\right)^{1/3}\left[\mathrm{Fr}/\mathrm{We}^{0.5}\right]. \tag{6}$$

The glossary of terms appears at the end of this document.

3.2. Calculation of temperature gradients of gaseous mixtures flowing through the injection lance

The temperature of the gaseous mixture at the inlet to the melt could be obtained with some inaccuracy from experimental data, if available; otherwise it might be determined by means of a heat balance in a small cylindrical control volume. In the present case, it was chosen to determine inlet temperature solving a differential equation describing the temperature gradient inside the concentric steel tube throughout the lance. Figure 2 shows the geometry of the control volume considered for calculating the temperature of the inlet gaseous mixtures.

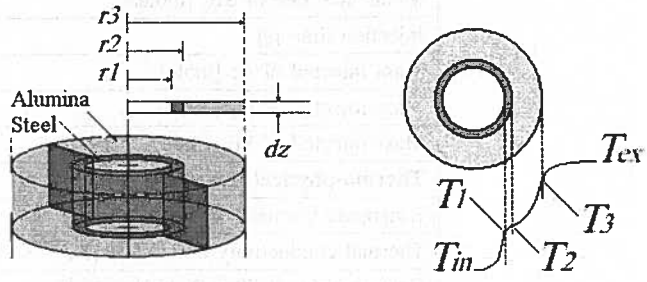

Fig. 2. Control volume considered to calculate the temperature acquired by a gaseous mixtures as it flows through injection

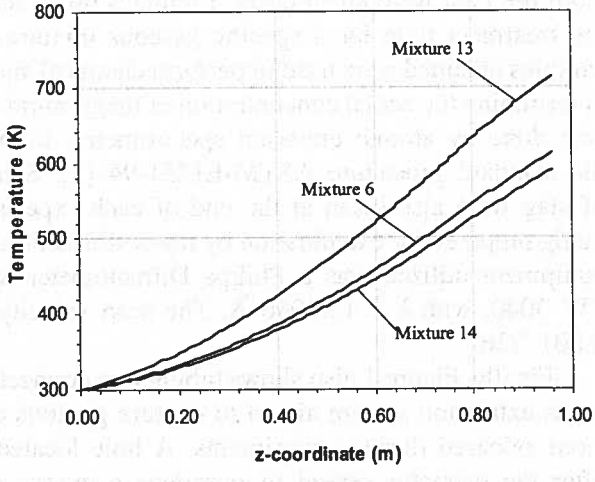

Fig. 3. Temperature gradients of each gaseous mixture flowing through lance 1. The injection conditions were Q_g = 20 L/min, P = 500 KPa

In turn, Figure 3 shows the temperatures calculated for the gaseous mixtures when they flew through the injection lance 1. These results are congruent with other theoretical values prediction [11]. In particular, when pure argon flew at 33×10^{-06} m^3/s at 500 KPa of pressure, the inlet temperature calculated was of 673 K. Therefore it

is valid to state that if the gas flow rate increases up to the values used in this work, the temperature of the gas flowing through lance 1 would be around 700 K. Taking this value as the inlet temperature to the system, the thermal conductivities and heat transfer coefficients must be evaluated at temperatures between the limits 300 and 700 K.

3.3. Chemical properties of gaseous mixtures as a function of temperature and pressure

In general, the thermal rupture of a covalent bond in a gas molecule causes the formation of atoms and free radicals chemically reactive, enhancing impurities oxidation rate in a molten phase. Thus, the reactivity of the gaseous mixtures containing SF_6(g) can be predicted on the basis of concentration of atoms and free radicals as a function of temperature [12]. For the present case it is possible to establish that the reactivity of the mixtures containing SF_6(g) depends chiefly on the atomic fluorine concentration. Figures 4 and 5 were obtained using the HSC software and show the change in chemical composition of two gaseous mixtures as a function of temperature at constant pressure. It is worth mentioning that for the plotting of these figures, inlet temperature of the gases was determined from Figure 3.

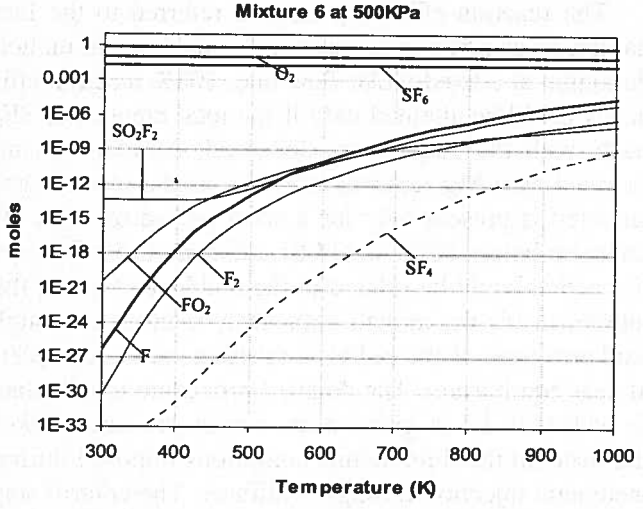

Fig. 4. Equilibrium data about thermal decomposition of the gaseous mixture number 06 at 500KPs

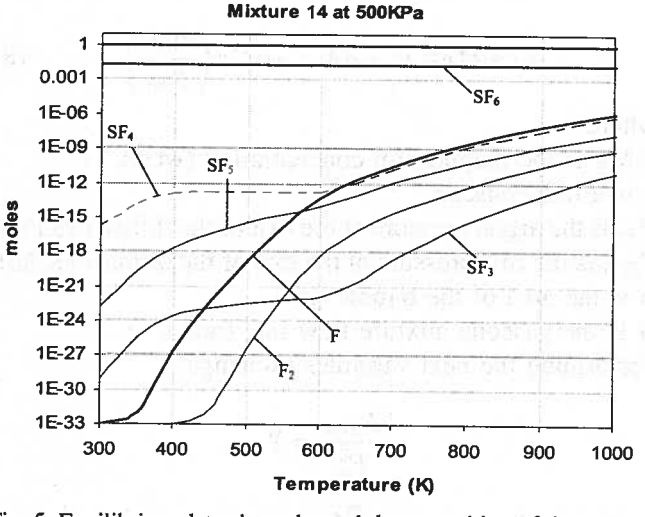

Fig. 5. Equilibrium data about thermal decomposition of the gaseous mixture number 14 at 500KPs

3.4. Experimental and theoretical study of the change in composition of the molten phase and evaluation of the kinetics of oxidation of magnesium dissolved in molten aluminum by Ar-SF_6 gaseous mixtures

Figure 6 shows the experimental results obtained after pneumatic injection of the gaseous mixtures at the temperature of 1023 K, pneumatically injected at 20 l/min. As it can be seen, different reaction yielding was obtained. From the technological point of view, suitable Mg removal rate results are obtained when using dilute Ar/SF_6 gaseous mixtures containing as low as 0.02 mole fraction of SF_6, no matter that injection time is enlarged. Nevertheless, in order to overcome enlarging treatment time, temperature or injection flow rate could be increased. Figure 7 shows the effect of temperature on the magnesium removal rate of Ar-2SF_6 gaseous mixtures pneumatically injected at 40 l/min. As it can be seen in this graph, levels of magnesium close to 0.1 wt.% could be reached in an elapsed time of just above 30 minutes at the temperature of the molten metal of 1048 K. The enhanced effect of temperature could be ex-

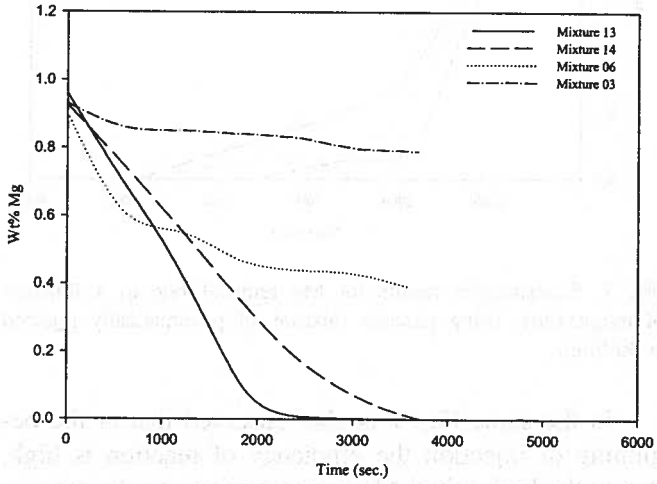

Fig. 6. Experimental results for Mg removal rate using the gaseous mixtures indicated, at T_L = 1023 K, pneumatically injected at 20 l/min

plained considering that magnesium diffusion increases when temperature increases, remaining more concentrated at the gas-liquid interphase. Moreover, reducing the surface tension of molten aluminum. However, the Gibbs adsorption equation indicates that the concentration of magnesium at the gas-liquid interphase decreases when temperature increases. This prediction shows the convenience of injecting the gaseous mixtures maintaining the temperature of molten metal at the lower value, but it can be taken into account that the selective oxidation depends on the increased migration of magnesium atoms towards the gas-molten metal boundary layer. Therefore, to compensate the effect of lowering the temperature, injection flow rate must be increased.

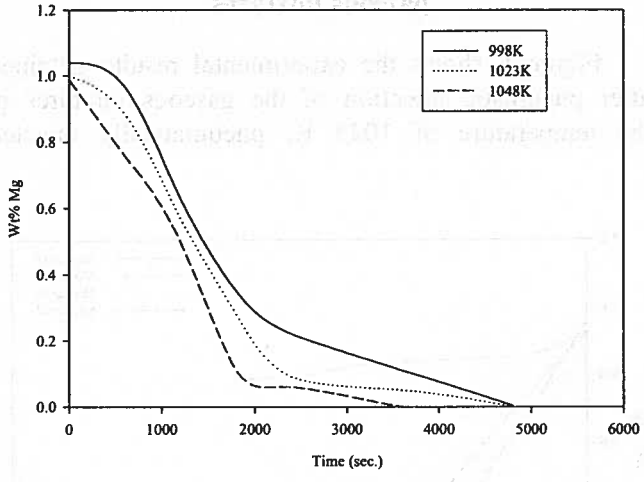

Fig. 7. Experimental results for Mg removal rate as a function of temperature, using gaseous mixture 14 pneumatically injected at 40 l/min

In the same Fig. 7 is also observed that at the beginning of injection the efficiency of reaction is high, due to the high initial Mg concentration. As the magnesium content is reduced significantly, i.e. periods of time above 30 min., the reaction efficiency is also reduced. A kinetic model could be developed for predicting magnesium removal rate at the conditions studied in this work, thus calculating activation energy and other kinetic parameters of interest.

In this part of the study a kinetic model for measuring magnesium removal rate when using Ar-SF_6 pneumatically injected is presented, which is based on the general ideas of Engh and Sigworth for molten aluminum refining using Ar/Cl_2 gaseous mixtures [13].

The basic considerations are the following:

1) Reaction rate is described by a second order kinetic equation where the control step is chemical reaction.
2) Simplifications arouse due to the small SF6 concentration in the gaseous phase flowing through the molten bath, i.e. 0.02 mole fraction.

Kinetic equation to be solved is the following:

$$\frac{W}{(100 * Aw_{Mg})}\frac{d(\%Mg)}{dt} = -\alpha G_{SF6} Ef, \tag{7}$$

where

W is the mass of molten metal (kg).
%Mg is the actual magnesium concentration (weight %).
Aw_{Mg} is the atomic weight of magnesium.
G_{SF6} is the molar flow rate of SF_6 (mol.s^{-1}).
Ef is the efficiency of reaction.
α value depends on the value of the stoichiometric coefficients. Taking as valid reaction R4 from Table I of the original paper, this value equals 2.

The reaction efficiency term is referred to the fact that if a given reactive gas species is injected into molten aluminum at a fixed molar flow rate, 100% reaction efficiency could be attained only if the total amount of SF_6 reacts with the magnesium dissolved, therefore giving the maximum Mg removal rate. But as the reactive gas delivered is present only for a short period of time, efficiencies below 100% could be attained. The efficiency of reaction could be related to the residence time of the bubbles inside the molten bath. Only if there is enough residence time of the bubbles, reaction can be completed near equilibrium. The detailed procedure to calculate the value of E_f is given next, whose procedure takes into account the fluidynamic conditions imposed during pneumatic injection through a diffuser. The control step considered is chemical reaction. A mass balance of the reaction of SF_6 with magnesium reaching the surface of a bubble is performed:

$$k\,(\%Mg)^2\,P_{SF6}dA = -\alpha G d\left(\frac{P_{SF6}}{P_{Ar}}\right), \tag{8}$$

where

%Mg is the magnesium concentration (wt%).
k is a rate constant.
P_{Ar} is the argon pressure at the exit of the diffuser (KPa.).
P_{SF6} is the SF_6 pressure at the exit of the diffuser (KPa.).
A is the area of the bubble (m^2).
G is the gaseous mixture flow rate (mol.s^{-1}).
Performing the next variables exchange:

$$\frac{P_{SF6}}{P_T^0} = Y$$

$$\frac{P_T}{P_T^0} = \eta \tag{9}$$

$$\upsilon = \frac{Y}{\eta},$$

where
P_T^0 is a reference pressure at the exit of the diffuser (KPa).
P_T is the total pressure in any point inside the molten bath (KPa).
Due to the low concentration of SF_6 in the gaseous mixture, $P_T = P_{Ar}$.
The differential of area could be calculated as follows:

$$dA = \pi d_B N e dh, \tag{10}$$

where
d_b is the average bubbles diameter (m), that can be determined using equation (6).
N is the total number of bubbles inside the system.
e is a bubbles shape factor, that in our case can be taken as 0.5.
h is the height of the molten bath (m).
The differential of height is given by:

$$d\eta = \frac{\rho g dh}{P_T^0}, \tag{11}$$

where ρ is the molten metal density ($kg.m^{-3}$).
g is the gravitational constant ($9.81 m.s^{-2}$).
The rising velocity of a bubble is given by:

$$u_B = \sqrt{\frac{g d_B}{2}} \tag{12}$$

while the total number of bubbles is given by:

$$N = \frac{n_B}{u_B} = \frac{n_B}{u_B^0}\sqrt{\frac{d_B^0}{d_B}}. \tag{13}$$

Here d_B^0 is the diameter of the bubbles at the exit of the diffuser, and nb is the number of bubbles at the same point. The increment of the volume of the bubbles is due basically to the pressure drop, so next expression is used:

$$\frac{V_B}{V_B^0} = \left(\frac{d_B}{d_B^0}\right)^3 = \frac{P_T^0}{P_T} = \frac{1}{\eta}. \tag{14}$$

V_b is the volume change of the bubbles during their ascension of the bubbles to the top of the molten bath (m^3).
V_B^0 is the initial volume of the bubbles volume at the exit of the diffuser (m^3).
Substitution of the equations written before in equation (1) gives the next differential equation:

$$\frac{d\upsilon}{\upsilon} = -k'(\%Mg)^2 \eta^{1/2} d\eta. \tag{15}$$

In this equation the value of the constant k' is calculated from:

$$k' = \frac{k\pi e n_B d_B^{0^2} P_T^{0^2}}{u_B^0 \alpha G \rho g}. \tag{16}$$

Substituting the value of k' and integrating equation (15) yields:

$$\ln\left(\frac{\upsilon}{\upsilon_0}\right) = -\frac{2}{3}k'(\%Mg)^2\left(\eta^{3/2} - \eta_0^{3/2}\right) = -k_2(\%Mg)^2. \tag{17}$$

Efficiency of the reaction therefore is given by:

$$E_f = 1 - \frac{\upsilon}{\upsilon_0} = 1 - \exp\left[-k_2(\%Mg)^2\right], \tag{18}$$

where k_2 could be considered as a rate constant whose units are 1/(wt%).
Finally, substituting the value of E_f in equation (7) we obtain:

$$\frac{W}{(100 * Aw_{Mg})}\frac{d(\%Mg)}{dt} = -\alpha G_{SF6}\left[1 - \exp\left(-k_2(\%Mg)^2\right)\right]. \tag{19}$$

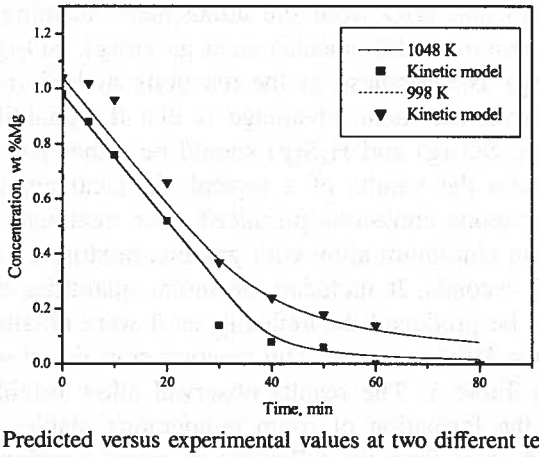

Fig. 8. Predicted versus experimental values at two different temperatures

This equation can not be solved analytically, so a numerical procedure must be employed. A numerical method was developed, finding the value of k_2 which permits to adjust the predicted values to the experimental values. This procedure is repeated for every temperature, so the values of k_2 could be used to evaluate the activation energy of the process. Figure 8 shows graphically how the experimental values and the values predicted by the kinetic model for two different temperatures, i.e. 998 and 1048 K, adjust. A good agreement is observed, therefore validating the utility of the kinetic model. On the other hand, from the values of k_2 determined to satisfy the adjustment of experimental to calculated values of the magnesium removal rate, an Arrhenius plot can

be drawn. Figure 9 shows such a graph, from whose slope a value of the activation energy of the process was obtained. This value equals 304.28 KJ/mol.

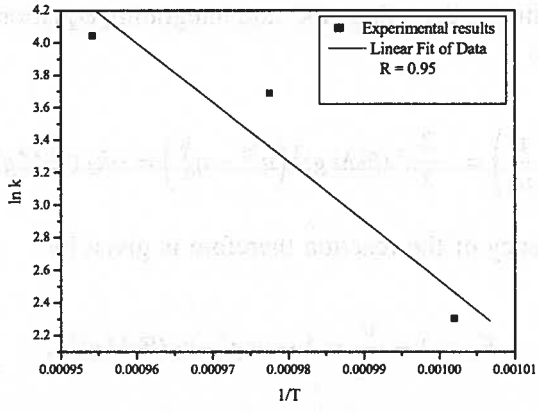

Fig. 9. Arrhenius plot for determination of Activation Energy of the Mg removal process using Ar-SF_6 gaseous mixtures

Most of the reactions considered in this work state that $SSF_2(g)$ is produced just after initiation of the reaction of dissolved Mg with SF_6. According to Figures 4 and 5, the predictions indicate that SF_6 decomposes into various sulfur fluorides and sulfur oxy-fluorides at high temperatures. On cooling, $SSF_2(g)$ reacts with oxygen and H_2O from the atmosphere, forming room temperature stable species such as HF(g), $SO_2(g)$ and $H_2S(g)$. Nevertheless, as the reactions studied are quite selective, the main advantage is that the quantities of HF(g), $SO_2(g)$ and $H_2S(g)$ should be rather low. Table 4 shows the results of a typical chemical analysis of the gaseous emissions produced after treatment of the molten aluminum alloy with gaseous mixture 13 during 3642 seconds. It includes the molar quantities expected to be produced theoretically, as it were obtained using the HSC software. The reaction considered was R8 from Table 1. The results observed allow establishing that the formation of room temperature stable species could come from the following chemical reaction:

$$3SSF_2(g) + 3/2O_2(g) + 5H_2O(g) \rightarrow 6HF(g) + 4SO_2(g) + 2H_2S(g) \quad (20)$$

Comparing the values of both experimentally analyzed and theoretically calculated values for the molar quantities of resultant gaseous emissions, it could be established that the oxidation of magnesium from molten aluminum by SF_6 is a quite efficient process.

TABLE 4
Experimental results and theoretical prediction about the gaseous emissions produced after pneumatic injection of mixture 13 during 3642 seconds

Gaseous species	HF	SO_2	H_2S
Total molar emission [mol/h]	5.35	9.71	3.16
Theoretical total molar emission, HSC [mol/h]	4.07	9.59	2.54

Regarding the use of Ar-O_2 gaseous mixtures, the results presented in Figure 6 show a low Mg removal rate, corresponding to an efficiency of only 24.76%. Campbell [14] stated that the molten aluminum oxidation by O_2 takes place slowly due to both a passivity effect of Al_2O_3 formation, and the extremely very low solubility of oxygen in molten aluminum. Nevertheless, adding oxygen to the Ar-SF_6 gaseous mixtures had the main effect not only in changing the composition of the emissions leaving the reaction system, but also reducing additionally the Gibbs free energy of reaction for about −249.16 KJ/mol-Mg. The fact that gaseous species formation such as HF, SO_2, or H_2S is taking place when using a gaseous mixture containing SF_6 plus O_2 suggests the possibility of using diluted aqueous solutions containing a chemical like CaO. This is to control the release of such a pollutant emissions, avoiding the formation of other fluorides such as SO_2F_2 or FO_2.

Figure 10 shows a typical X-ray diffraction pattern of a slag including the compounds identified, corresponding to the bubbling of the gaseous mixture 6 after 3608 seconds at the temperature of 1023K. This pattern shows the presence of $MgAl_2O_4$, MgF_2, α-Al_2O_3, Al, AlN, and other complex oxides of aluminum and magnesium. $MgAl_2O_4$ is formed by reaction between Al_2O_3 and MgO according to reaction R7 from Table 1. MgF_2 is formed according to reaction R4 of Table 1, while AlN was produced by a high temperature reaction between molten aluminum and the nitrogen of the atmosphere.

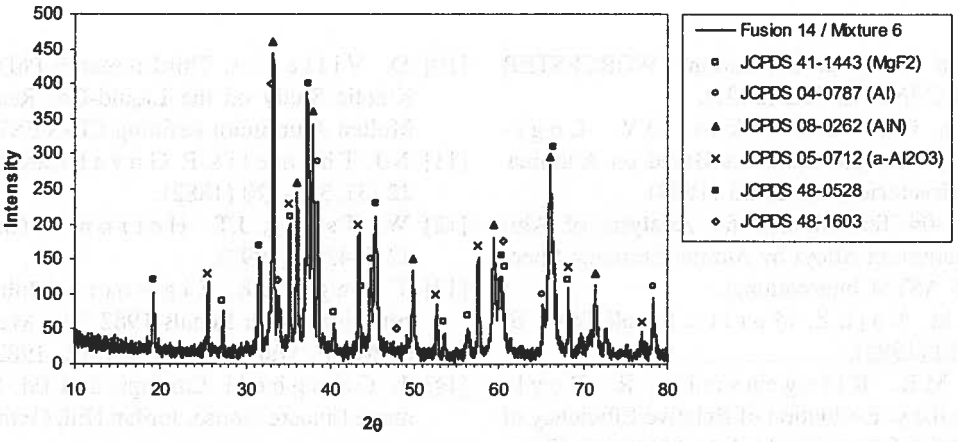

Fig. 10. X-ray diffraction pattern of a sample of slag obtained during bubbling of the gaseous mixture 6 at 1023 K.
JCPDS 48-0528 corresponds to $MgAl_2O_4$ (Magnesium Aluminum Oxide).
JCPDS 48-1603 corresponds to $MgSi_{1.67}Al_{2.47}O_{3.19}N_{3.81}$ (Magnesium Aluminum Silicon Oxide Nitride).

4. Conclusion

From chemical analysis of residual magnesium in the alloys, the chemical composition of the slag produced, and of the gaseous emissions released, it is possible to propose a scheme of reaction for magnesium refining from molten aluminum using Ar-SF_6-O_2 gaseous mixtures. The main reaction is shown in bold letters, while by-products formation is explained by the reactions shown by the vertically oriented arrows.

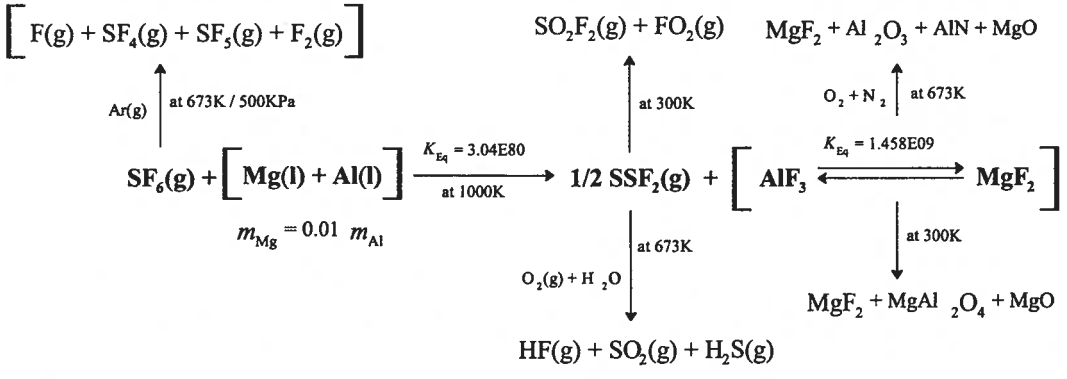

The magnesium oxidation process using Ar-SF_6 gaseous mixtures used in this work were quite selective, so the small amounts of gaseous species released such as SO_2, H_2S or HF could be controlled properly by a chemical neutralization stage.

Acknowledgements

The authors wish to thank the National Science and Technology Council of México (CONACYT) for the financial support provided, project 38466U and scholarship 139525. The scientific support of Dr. Janusz Donizak of the University of Mining and Metallurgy of Krakow, Poland is acknowledged. Finally, PRAXAIR México® for the technical and economical support and for providing the gaseous mixtures.

REFERENCES

[1] David V. Neff, Brian P. Cochran, Chlorination Technology in Aluminum Recycling. Light Metals 1993, 1053-1060 (1993).

[2] Baozhong Zhao, Nickolas J. Themelis, Kinetic Study of As, Sb and Bi Removal from Copper by SF_6 Injection. Gas Interactions in Nonferrous Metals Processing, The Minerals, Metals & Materials Society, 127-143 (1996).

[3] P. Waite, D. Bernard, Recent Experience with the Use of Sulphur Hexafluoride for Aluminum Fluxing. Light Metals 1990, 1053-1060 (1990).

[4] Roine, Outokumpu HSC Chemistry for Windows. Outokumpu Research Company, Pori, Finland, (1993).

[5] Virendra S. Warke, M.C. Thesis, Removal of Hydrogen and Solid Particles from Molten Aluminum Alloys in the Rotating Impeller Degasser: Mathemati-

cal Models and Computer Simulations. WORCESTER POLYTECHNIC INSTITUTE (2003).
[6] E.S. Lukin, O.V. Gorshkov, O.V. Logina, Porous High-strength Ceramics Based on Alumina. Ogneupori (Refractories) **10**, 23-25 (1989).
[7] ASTM; E1251-04 Test Method for Analysis of Aluminum and Aluminum Alloys by Atomic Emission Spectrometry, 2005 ASTM International.
[8] M. Iguchi, M. Kaji, Z. Morita, Metall Trans. B; **29B**, 1209-1218 (1998).
[9] Q.T. Fang, M.K. Klingensmith, R. Boylstein, L. Podey, Evaluation of Relative Efficiency of Various Degassing Lances for Molten Aluminum Treatment Applications Light Metals 2004, 737-742 (2004).
[10] D. Villegas, Third research PhD Thesis report; A Kinetic Study on the Liquid-Gas Reactions Applied to Molten Aluminum Refining CINVESTAV-Saltillo, 2005.
[11] N.J. Themelis, P. Goyal, Canadian Metall. Quart., **22** (3), 313-320 (1882).
[12] W. Tsang, J.T. Herron, J. Chem. Phys., **96**(6), 4272-4282 (1992).
[13] T. Engh, G.K. Sigworth, Molten Aluminum Purification. Light Metals 1982, The Metallurgical Society of AIME, Warrendale, PA, USA, 1982, 983-1001.
[14] J. Campbell, Castings, 2nd Ed. Butterworth-Heinemann Linacre House, Jordan Hill, Oxford, 4-5, UK, 2001.

Received: 10 February 2006.